DOI: 10.3901/CJME.2015.0302.022, available online at www.springerlink.com; www.cjmenet.com; www.cjme.com.cn

Analysis and Numerical Simulation of Rolling Contact between Sphere and Cone

ZHAO Yanling[1,*], XIA Chengtao[1], WANG Hongbo[2], XUAN Jiaping[2],
XIANG Jingzhong[1], LIU Xianli[1], and SU Xiangguo[1]

1 *School of Mechanical and Power Engineering, Harbin University of Science and Technology, Harbin 150080, China*
2 *Shenyang Aerospace Mitsubishi Motors Engine Manufacturing Co., Ltd, Shenyang 110000, China*

Received December 18, 2014; revised February 26, 2015; accepted March 2, 2015

Abstract: In non-conforming rolling contact, the contact stress is highly concentrated in the contact area. However, there are some limitations of the special contact model and stress model used for the theoretical study of the phenomenon, and this has prevented in-depth analysis of the associated friction, wear, and failure. This paper is particularly aimed at investigating the area of rolling contact between a sphere and a cone, for which purpose the boundary is determined by the Hertz theory and the geometries of the non-conforming surfaces. The phenomenon of stick-slip contact is observed to occur in the contact area under the condition of no-full-slip ($Q < \mu \bullet P$). Using the two-dimensional rolling contact theory developed by CARTER, the relative positions of the stick and slip regions and the distribution of the tangential force over the contact area are analyzed. Furthermore, each stress component is calculated based on the McEwen theory and the idea of narrow band. The stress equations for the three-dimensional rolling contact between the sphere and the cone are obtained by the principle of superposition, and are used to perform some numerical simulations. The results show that the stress components have a large gradient along the boundary between the stick and slip regions, and that the maximum stress is inversely proportional to the contact coefficient and proportional to the friction coefficient. A new method for investigating the stress during non-classical three-dimensional rolling contact is proposed as a theoretical foundation for the analysis of the associated friction, wear, and failure.

Keywords: tractive rolling, Hertz theory, stick-slip contact, contact area, contact stress

1 Introduction

When two non-conforming solids come into non-deformation contact, an initial point or line of contact is formed. A limited contact area is thereafter generated under a normal force. The contact area is far less than the size of contacting objects, and the contact stress is highly concentrated. Although the contact area is very small, in the field of contact mechanics, it is essential to determine its scope and the stress state within it, and this has always been a hot issue in engineering[1].

The Hertz theory is usually used to determine the scope of the contact area and as a basis for analyzing the stress state within it[2–4]. However, one of the crucial constraints in the application of the Hertz theory is that it assumes that the contact between the two solids involves only a normal force, without the presence of tangential friction. This is not in conformity with the practical situation. Nonetheless, with properly consideration of the friction in the area, the Hertz theory can be widely applied to sliding and rolling contact problems in a more practical way. SACKFIELD, et al discussed the Hertz contact problems under classic[5] and tangential load[6] conditions, and summarized the stress state under different contact forms. ZHUPANSKA, et al[7], investigated the effect of the tangential stress on the normal stress when a cylinder slides on a half-flat under friction, and presented the exact solution of the stress distribution in the contact region in the form of a hypergeometric function. GOODMAN[8] and SPENCE[9] posited that the interaction between the tangential and normal forces on the contact surface could be neglected. This proposition was deeply analyzed by JOHNSON[10], who proved that the mutual effect of the tangential and normal forces for the deformation and stress are very small and could be considered to be independent, thus enabling independent calculation of the total stress by superposition of the different stress components. SHCHERBAKOV[11] exactly derived the stress state by superposition of the stress fields induced by the normal and tangential contact loads, which were considered to be elliptically distributed. The idea of superposition is also employed in the stress calculation of this paper.

CARTER[12] and FROMN[13], whose ideas and research methods founded and gave direction to the study of three-dimensional rolling contact theory, analyzed two-dimensional

* Corresponding author. E-mail: zhaoyanling@sina.com
Supported by National Natural Science Foundation of China(Grant No. 51275140)

elastic rolling contact using the Hertz and elastic half-space theories. The non-Hertz three-dimensional elastic rolling contact theory and the associated CONTACT program were later proposed by KALKER[14]. These have been widely used in the analysis of wheel/rail contact[15–21], in the process of which they have also been continuously improved. The finite element method and the corresponding software have been used by many researchers to analyze mechanical behavior[22–26]. Regarding the characterization of the relevant details, the simultaneous existence of the stick and slip regions was first experimentally discovered by Raynolds, and the slip region was thought to expand until the occurrence of gross sliding. The condition of partial-stick and partial-slip is also generated during the initial sliding contact of two solids. The basic principles and research methods for stick-slip contact were later proposed by JOHNSON[10], and the numerical solution was obtained by MAOUCHEN, et al[27]. The finite element model, which is based on the robust cyclic plasticity theory, was used by XU, et al[28] to simulate the elastic-plastic stresses of partial slip-line rolling contact. They showed that the partial slip condition significantly affected the stress in the rolling direction, but not that in the axial direction. LEE, et al[29], studied the steady-state and transient rolling contact problems of three-dimensional elastic bodies and the three-dimensional distribution of the tangential traction and contact stresses in the contact area, and explained the effect of the stick-slip region. ETSION, et al[30], experimentally demonstrated the process of the variation of the frictional force between initial partial sliding and gross sliding.

Some limitations still exist in the analysis of the behavior of rolling contact. Firstly, the analysis models are mainly for contacts between a cylinder and a plane, between two cylinders, between a sphere and a flat, and between two spheres. There are no models for some special contact cases encountered in engineering practice. Secondly, in recent years, experiments and finite element methods have been mostly used to investigate stress, and the theoretical analysis of rolling contact is rarely undertaken. Based on the achievements of previous theoretical studies, three-dimensional elastic rolling contact between a steel ball and a control wheel, which is crucial to automatic detection equipment detecting steel balls, is investigated in this paper. The geometric size of the contact area is determined and some novel methods and ideas are used to analyze the stress state in the rolling contact area in a step-by-step manner. This is done to obtain analytic solutions of the stresses and determine the characteristics of each stress component.

2 Scope of Rolling Contact Area

2.1 Analytic model

Tractive rolling contact between a steel ball and a control wheel is crucial to automatic detection equipment detecting steel balls, and is a typical example of three-dimensional non-conforming rolling contact between a sphere and a cone. The contact is depicted in Fig. 1. Under the normal force P', the steel ball and bilateral cones of the control wheel are brought together. Under the driving torque, the steel ball rotates about the axis AB, thereby causing the control wheel to rotate about the fixed axis CD. It is assumed that P is a normal force between the sphere and the one-side cone, with its direction passing through the center of the sphere (point O' in Fig. 1) and the initial contact point (point o in Fig. 1).

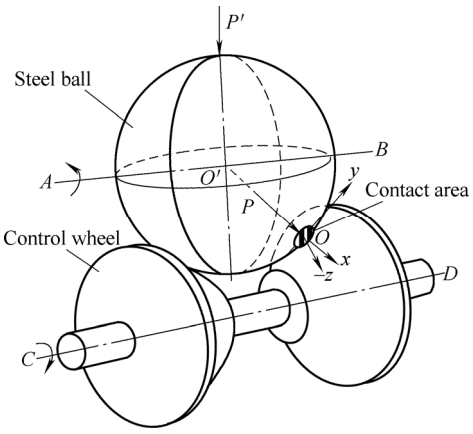

Fig. 1. Tractive rolling contact between steel ball and control wheel

The contact surface is generated between the sphere and one side of the cone under the normal force P, and is considered to be an ellipse based on Hertz theory. The contact area is exaggerated in Fig. 1, and its actual dimensions in engineering practice are quite small, based on which the coordinate system is established. Following are descriptions of how to determine the geometric dimensions of the contact area and the analysis formulas of the stress.

2.2 Calculation of contact area

The general elliptical shape of the contact area was proposed by Hertz based on experimental observation of the interference fringes. He also introduced the simplification of each of the contacting bodies being an elastic half-space, and of the force acting on a flat surface in the small elliptical contact area. Based on these simplifications, the distribution of the normal pressure $p(x, y)$ in the contact area can be expressed as

$$p(x,y) = p_0\left(1 - x^2/a^2 - y^2/b^2\right)^{1/2}. \tag{1}$$

The boundary equation of the elliptical contact surface is as follows:

$$x^2/a^2 + y^2/b^2 - 1 = 0, \tag{2}$$

where p_0 is the maximum contact pressure and a and b

respectively denote the minor and major semi-axes of the ellipse. Analysis based on the Hertz theory shows that the eccentricity ratio of the ellipse is independent of the loads and only depends on the relative radii of the surface curvatures of the two contacting bodies at the initial contact point. The relative radii of the curvatures can be calculated based on the geometry of the smooth non-conforming contact surface. Based on the geometry, the initial gap between the two curved surfaces can also be expressed as follows in terms of the relative radii of the curvatures near the initial contact point:

$$h=\frac{1}{2R'}x^2+\frac{1}{2R''}y^2, \tag{3}$$

where R' and R'' are the relative radii of the curvatures of the sphere and the cone at the contact point, respectively. According to the geometrical characteristics of a sphere and a cone, the relative radii can be obtained as

$$R_1'=R_1''=R_1, \tag{4}$$

$$R_2'=\infty,\ \ R_2''=R_2, \tag{5}$$

where R_1 is the radius of the sphere; R_1' and R_1'' are respectively the main radii of the curvatures of the sphere and the cone at the initial contact point; R_2' is a main radius of curvature of the cone, the value of which tends to infinity; and R_2'' is another radius of curvature of the cone, and is defined as R_2 for convenience. Eq. (4) can be obtained based on the symmetry of a sphere. For a cone angle of $\pi/2$, R_2 is numerically equal to the distance between the contact point and the vertex of the cone in the bus direction. The relevant relationships are as follows:

$$1/R'=1/R_1'+1/R_2', \tag{6}$$

$$1/R''=1/R_1''+1/R_2'', \tag{7}$$

From Eqs. (4)–(7), the relative radii of curvature of the sphere and the cone can be obtained as

$$R'=R_1, \tag{8}$$

$$R''=R_1R_2/(R_1+R_2), \tag{9}$$

From Eqs. (8) and (9) and the Hertz theory, the parameters b, a, and p_0 can be obtained as

$$b=\left(\frac{3P}{4E^*}\right)^{1/3}\left[\frac{R_1^2(R_1+R_2)}{R_2^2}\right]^{1/6}, \tag{10}$$

$$a=\left(\frac{3P}{4E^*}\right)^{1/3}\left[\frac{R_1^2R_2^2}{(R_1+R_2)^3}\right]^{1/6}, \tag{11}$$

$$p_0=\left(\frac{6PE^{*2}}{\pi^3}\right)^{1/3}\left(\frac{R_1+R_2}{R_1^2R_2}\right)^{1/3}, \tag{12}$$

where

$$\frac{1}{E^*}=\frac{1-\nu_1^2}{E_1}+\frac{1-\nu_2^2}{E_2}. \tag{13}$$

Where ν_1, E_1, ν_2, and E_2 are respectively the Poisson's ratio and Young's modulus of the materials of the sphere and the cone, from which the equivalent modulus of elasticity E^* is obtained.

It should be emphasized that the computer mode proposed by JOHNSON[10] is used for Hertz theory calculations. This eliminates the need to evaluate integrals or rather complicated functions. That is, the relationship between the correlative ellipse integral functions and the value of R_2/R_1 is expressed by several curves, which can be used to obtain the required values.

3 Calculation of Stress State

3.1 Distribution of forces

Based on the rolling contact theory, the tangential force at the boundary of the contact area tends to infinity while the normal force tends to zero. Hence, the contact condition ($Q < \mu \bullet P$) cannot be satisfied and gross sticking could not occur, resulting in relative sliding even if the tangential force is very small. Between the boundary and the center of the contact area, the normal force (based on the distribution expressed by Eq. (1)) gradually increases while the tangential force gradually decreases. There must thus be a critical boundary inside which the stick phenomenon occurs where the stick condition is satisfied, and outside which slipping occurs where the tangential force exceeds the limiting friction. Hence the stick-slip situation occurs in the contact area under the combined effect of the tangential and normal forces.

In rolling contact between a sphere and a cone, one side of the contact area close to the rolling direction is under compression and the other side is under tension. The stick region therefore shifts in the rolling direction and the offset distances of all the point are equal. It is only at the boundary of the stick region (y=0) that the offsets coincide with the contact boundary owing to the special geometric area of the ellipse as discussed in Eqs. (1) and (2). The elliptical contact area is defined on the x-y plane, where o is the origin and initial contact point, and the x- and y-axis coincide with a and b as discussed earlier in connection with Fig. 1. The y-axis is in the direction of the cone generatrix, and the sphere rolls in the negative direction of the x-axis. The reversed z-axis is perpendicular to the x-y plane and points inwards of the cone in the rectangular coordinate system. As shown in Fig. 2, c and d denote the semi-axes of the elliptical stick region, which has its midpoint at o' and an offset distance of s.

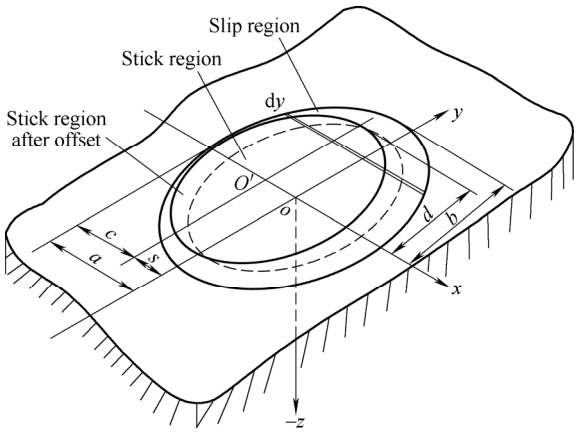

Fig. 2. State of contact area under rolling contact

With regard to the distribution of the tangential force, POPOV[31] used similar steps and assumptions as those proposed by CARTER[12] to calculate the three-dimensional stress state in the rolling contact area of the sphere and plane. The same procedure was adopted in the present study to obtain the distribution of the tangential force in the three-dimensional rolling contact area. This was done by superposition of two types of "Hertz" stresses as follows:

$$q=\begin{cases}q'(x,y), & \text{slip region,}\\ q'(x,y)+q''(x,y), & \text{stick region,}\end{cases} \tag{14}$$

where

$$q'=\mu p_0\left[1-\left(\frac{x}{a}\right)^2-\left(\frac{y}{b}\right)^2\right]^{\frac{1}{2}}, \tag{15}$$

$$q''=-\frac{c}{a}\mu p_0\left[1-\left(\frac{x+s}{c}\right)^2-\left(\frac{y}{d}\right)^2\right]^{\frac{1}{2}}, \tag{16}$$

$$\left(\frac{x+s}{c}\right)^2+\left(\frac{y}{d}\right)^2\leqslant 1, \tag{17}$$

$$s=a-c. \tag{18}$$

Where q denotes the distribution of the entire tangential force, which is defined within the boundary given by Eq. (2); and q' and $(q'+q'')$ denote the distributions of the tangential force in the slip and stick region respectively.

3.2 Calculation of stress state

Based on the two-dimensional contact model of two cylinders with parallel axes under a normal force, MCEWEN calculated the stress components at any point (x, z) in the strip contact area, the width of which is constant in the axis direction. However, the width of the contact area of a sphere and cone varies in the y-axis direction, as shown in Fig. 2. In the present study, the elliptical contact area was divided into numerous narrow bands dy (see in Fig. 2), and the corresponding contact width is 2x, where

$$x=a\sqrt{1-\frac{y^2}{b^2}}. \tag{19}$$

The two-dimensional theory of cylindrical contact proposed by MCEWEN was applied to each narrow band dy and the interaction with the adjacent narrow band was neglected. The stress components of each narrow band under only a normal force can thus be expressed as

$$(\sigma_x)_p=-p_0\sqrt{1-\frac{y^2}{b^2}}\cdot\frac{1}{a\sqrt{1-\frac{y^2}{b^2}}}\cdot\left[m\left(1+\frac{z^2+n^2}{m^2+n^2}\right)-2z\right]=$$
$$-\frac{p_0}{a}\left[m\left(1+\frac{z^2+n^2}{m^2+n^2}\right)-2z\right], \tag{20}$$

$$(\sigma_z)_p=-p_0\sqrt{1-\frac{y^2}{b^2}}\cdot\frac{1}{a\sqrt{1-\frac{y^2}{b^2}}}\cdot m\left(1-\frac{z^2+n^2}{m^2+n^2}\right)=$$
$$-\frac{p_0}{a}m\left(1-\frac{z^2+n^2}{m^2+n^2}\right), \tag{21}$$

$$(\tau_{xz})_p=p_0\sqrt{1-\frac{y^2}{b^2}}\cdot\frac{1}{a\sqrt{1-\frac{y^2}{b^2}}}\cdot n\left(\frac{m^2-z^2}{m^2+n^2}\right)=$$
$$\frac{p_0}{a}n\left(\frac{m^2-z^2}{m^2+n^2}\right), \tag{22}$$

where

$$m^2=\frac{1}{2}\left[\left(a^2(1-\frac{y^2}{b^2})-x^2+z^2\right)^2+4x^2z^2\right]^{\frac{1}{2}}+$$
$$\frac{1}{2}\left(a^2(1-\frac{y^2}{b^2})-x^2+z^2\right), \tag{23}$$

$$n^2=\frac{1}{2}\left[\left(a^2(1-\frac{y^2}{b^2})-x^2+z^2\right)^2+4x^2z^2\right]^{\frac{1}{2}}-$$
$$\frac{1}{2}\left(a^2(1-\frac{y^2}{b^2})-x^2+z^2\right). \tag{24}$$

Where subscript p corresponds to the normal force.

Under sliding contact with interaction between the

tangential and normal forces, the stress relationship can be expressed as

$$\frac{(\sigma_x)_p}{p_0}=\frac{(\tau_{xz})_q}{q_0}, \tag{25}$$

$$\frac{(\tau_{xz})_p}{p_0}=\frac{(\sigma_z)_q}{q_0}, \tag{26}$$

where subscript q corresponds to the tangential force acting on the entire contact area; and q_0 is the tangential force corresponding to p_0, and is considered to be equal to μp_0. q' under rolling contact has the same distribution as q under sliding contact, but an opposite direction. The stress components $(\sigma_z)_{q'}$ and $(\tau_{xz})_{q'}$ can be calculated using Eqs. (20), (22), (25), and (26), and only $(\sigma_x)_{q'}$ needs to be calculated separately. The stress components induced by the tangential force q' in the contact area can be expressed as follows:

$$(\sigma_x)_{q'}=-(\sigma_x)_q=-\frac{\mu p_0}{a}\left[n\left(2-\frac{z^2-m^2}{m^2+n^2}\right)-2x\right], \tag{27}$$

$$(\sigma_z)_{q'}=-(\sigma_z)_q=-\frac{\mu p_0}{a}n\left(\frac{m^2-z^2}{m^2+n^2}\right), \tag{28}$$

$$(\tau_{xz})_{q'}=-(\tau_{xz})_q=\frac{\mu p_0}{a}\left[m\left(1+\frac{z^2+n^2}{m^2+n^2}\right)-2z\right]. \tag{29}$$

From Eqs. (15) and (16), the distribution of q'' is only defined in the stick region, and is similar to that of q', satisfying a certain proportion relationship. The parameter k is defined as the contact coefficient, where $c/a=d/b=k$. The axis of symmetry of the stick region is at $x=s$, and the stress components due to $q''(x)$ can thus be expressed as

$$(\sigma_x)_{q''}=\frac{\mu p_0}{c}\left[n^*\left(2-\frac{z^2-m^{*2}}{m^{*2}+n^{*2}}\right)-2(x+s)\right], \tag{30}$$

$$(\sigma_z)_{q''}=\frac{\mu p_0}{c}n^*\left(\frac{m^{*2}-z^2}{m^{*2}+n^{*2}}\right), \tag{31}$$

$$(\tau_{xz})_{q''}=-\frac{\mu p_0}{c}\left[m^*\left(1+\frac{z^2+n^{*2}}{m^{*2}+n^{*2}}\right)-2z\right], \tag{32}$$

where

$$m^{*2}=\frac{1}{2}\left[\left(c^2\left(1-\frac{y^2}{d^2}\right)-(x+s)^2+z^2\right)^2+4(x+s)^2z^2\right]^{\frac{1}{2}}+\frac{1}{2}\left(c^2\left(1-\frac{y^2}{d^2}\right)-(x+s)^2+z^2\right), \tag{33}$$

$$n^{*2}=\frac{1}{2}\left[\left(c^2\left(1-\frac{y^2}{d^2}\right)-(x+s)^2+z^2\right)^2+4(x+s)^2z^2\right]^{\frac{1}{2}}-\frac{1}{2}\left(c^2\left(1-\frac{y^2}{d^2}\right)-(x+s)^2+z^2\right). \tag{34}$$

According to the results obtained by JOHNSON for a problem involving a tangential force, the stresses and deformations caused by the tangential and normal forces are independent of each other and the total stress can be obtained by superposition of the stress components.

The dimensionless analytic equations are here introduced to express the stress components in the contact area, using $W=x/a$, $H=y/b$, and $B=z/a$. By the superposition of Eqs. (20), (27), and (30), the stress component σ_x/p_0 can be obtained as

$$\frac{\sigma_x}{p_0}=\frac{(\sigma_x)_p}{p_0}+\frac{(\sigma_x)_{q'}}{p_0}+\frac{(\sigma_x)_{q''}}{p_0}=\frac{1}{\sqrt{1-H^2}}\left[Q\frac{B^2+T^2}{Q^2+T^2}-\mu T\frac{B^2-Q^2}{Q^2+T^2}+Q+2\mu T-2(B+\mu W)\right]-\frac{\mu}{\sqrt{k^2-H^2}}\left[T\left(2-\frac{B^2-Q^{*2}}{Q^{*2}+T^{*2}}\right)-\frac{k(1+W-k)}{\sqrt{k^2-H^2}}\right]. \tag{35}$$

In addition, by the superposition of Eqs. (21), (28), and (31), the stress component σ_z/p_0 can be obtained as

$$\frac{\sigma_z}{p_0}=-\frac{1}{\sqrt{1-H^2}}\left[Q-Q\frac{B^2+T^2}{Q^2+T^2}-\mu T\frac{B^2-Q^2}{Q^2+T^2}\right]-\frac{\mu}{\sqrt{k^2-H^2}}\left[T^*\frac{Q^{*2}-B^2}{Q^{*2}+T^{*2}}\right]. \tag{36}$$

Furthermore, by the superposition of Eqs. (22), (29), and (32), the stress component τ_{xz}/p_0 can be obtained as

$$\frac{\tau_{xz}}{p_0}=\frac{1}{\sqrt{1-H^2}}\left[T\frac{Q^2-B^2}{Q^2+T^2}-\mu Q\frac{B^2+T^2}{Q^2+T^2}-\mu Q\right]+\frac{\mu}{\sqrt{k^2-H^2}}\left[Q^*\frac{B^2+T^{*2}}{Q^{*2}+T^{*2}}+Q^*-2B\right]. \tag{37}$$

Where

$$Q^2=\frac{m^2}{a^2}=\frac{1}{2}\left[\left(1-H^2-W^2+B^2\right)^2+4x^2z^2\right]^{\frac{1}{2}}+\frac{1}{2}\left(1-H^2-W^2+B^2\right)^2, \tag{38}$$

$$T^2=\frac{n}{a^2}^2=\frac{1}{2}\left[\left(1-H^2-W^2+B^2\right)^2+4x^2z^2\right]^{\frac{1}{2}}-\frac{1}{2}\left(1-H^2-W^2+B^2\right)^2, \tag{39}$$

$$Q^{*2}=\frac{m^{*2}}{c^2}=\frac{1}{2}\left[\left(1-\frac{H^2}{k^2}-W^2+B^2\right)^2+4\left(x+s\right)^2z^2\right]^{\frac{1}{2}}+\frac{1}{2}\left(1-\frac{H^2}{k^2}-W^2+B^2\right)^2, \tag{40}$$

$$T^{*2}=\frac{n^*}{c^2}^2=\frac{1}{2}\left[\left(1-\frac{H^2}{k^2}-W^2+B^2\right)^2+4\left(x+s\right)^2z^2\right]^{\frac{1}{2}}-\frac{1}{2}\left(1-\frac{H^2}{k^2}-W^2+B^2\right)^2. \tag{41}$$

4 Numerical Simulation and Discussion

The stress components at any point within $z<0$ or on the surface of the contact area ($z=0$) can be determined using Eqs. (35)–(37). The characteristics of the latter are the focus of the present study. These characteristics have been previously determined by numerical simulation using the mathematical software MATLAB, and discussed in detail. The dimensionless forms of the coordinates are used in the following figures to present universal results. The three-dimensional distributions of the stresses σ_x/p_0, σ_z/p_0, and τ_{xz}/p_0 are shown in Figs. 3–5, respectively. The contact coefficient k and friction coefficient μ are the main factors that determine the stress components σ_x/p_0, σ_x/p_0, and τ_{xz}/p_0 obtained by Eqs. (36)–(37). The effects of different values of k and μ on the stress components are shown two-dimensionally in Figs. 6–8.

Fig. 3 shows the variation of the stress component σ_x/p_0 for $k=0.8$ and $\mu=0.15$ when the body is rolling in the negative direction of axis x/a and the width of the contact area changes along axis y/b. The offset of the stress in the rolling direction is shown in Fig. 3(a). It can be observed from Fig. 3(b) that the stress is compressive in the rolling direction and tensile in the opposite direction and that the amplitude of the compressive stress is larger than that of the tensile stress. However, because compressive stress is generally more likely to cause failure, both the largest compressive and tensile stresses should be taken into consideration in estimating the surface failure and checking the intensity. The phenomenon of stress mutation occurs at the boundary between the stick region and the slip region, resulting from the adopted CARTER[12] theory, as expressed by Eq. (14), in which the distributed force in the stick region is the algebraic sum of the slipping contact stress and its associated stress shrinking by a certain ratio relative to the contact coefficient, but in a reverse direction. In other words, the discontinuously distributed force in the contact area contributes to stress mutation, which is characteristic of a large-gradient stress in actual contact.

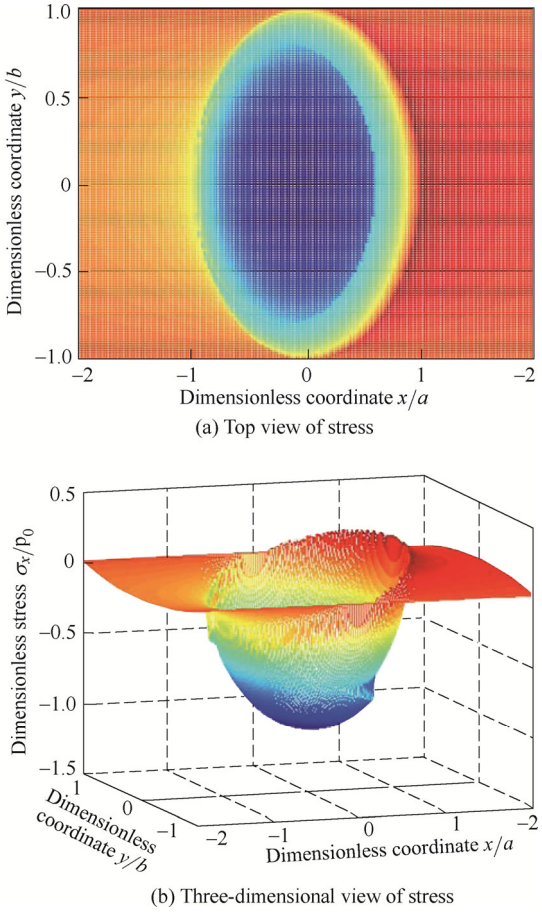

Fig. 3. Distribution of dimensionless stress σ_x/p_0 for $k=0.8$ and $\mu=0.15$

Figs. 4(a) and (b) show the variation of σ_z/p_0 when $k=0.8$ and $\mu=0.15$ for a surface contact area in which there is only compressive stress, the maximum value of which occurs at $x/a=0$. The distribution of σ_z/p_0 in the dimensionless coordinate system is hemispherical, and there is no stress mutation. Only the maximum compressive stress should thus be considered in a failure analysis.

Figs. 5(a) and (b) show the variation of τ_{xz}/p_0 for $k=0.8$ and $\mu=0.15$. It can be clearly observed from the figures that the stress in the slip region is greater than that in the stick region, for which reason the slip region is more susceptible to wear. In addition, stress mutation occurs at the junction of the stick and slip regions, and this should be considered in the numerical prediction of fatigue and analysis of failure.

Fig. 6(a) is a two-dimensional representation of the stress σ_x/p_0 for fixed values of $\mu=0.15$ and $y/b=0$ and varying values of k. It can be observed that, when $k=1$, the stick region covers the entire area, and there is no sliding or stress mutation. Although this is an ideal situation, it is impractical. When $k<1$, stress mutation occurs due to the

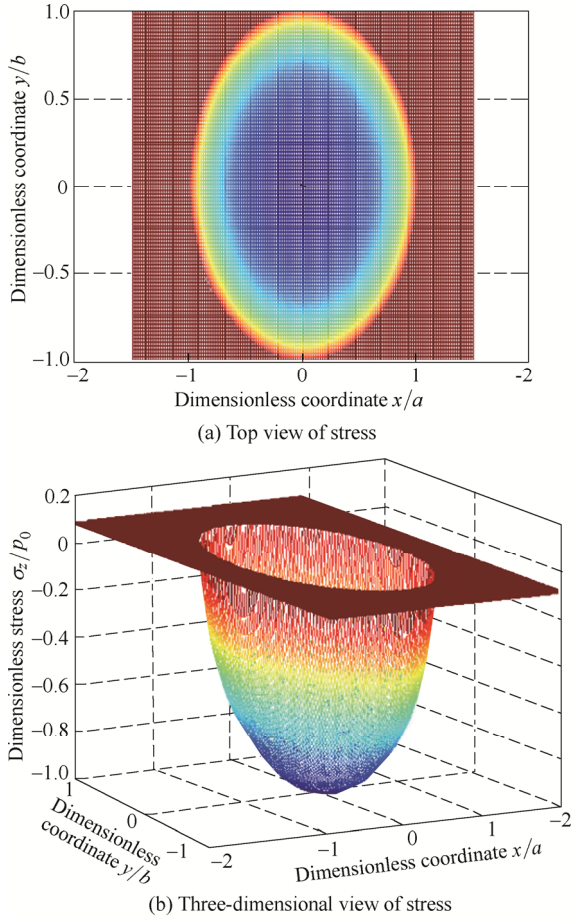

Fig. 4. Distribution of dimensionless stress σ_z/p_0 for k=0.8 and μ=0.15

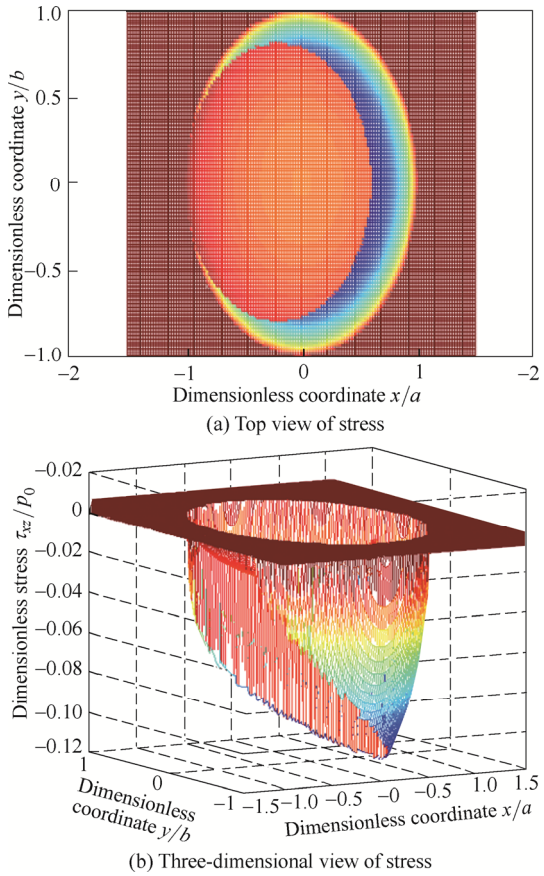

Fig. 5. Distribution of dimensionless stress τ_{xz}/p_0 for k=0.8 and μ=0.15

co-existence of stick and slip regions, and the stick region decreases with decreasing value of k. Fig. 6(b) shows that, for fixed values of k=0.8 and y/b=0, the tensile and compressive values of the stress σ_x/p_0 both increase with increasing μ, and stress mutation is more obvious.

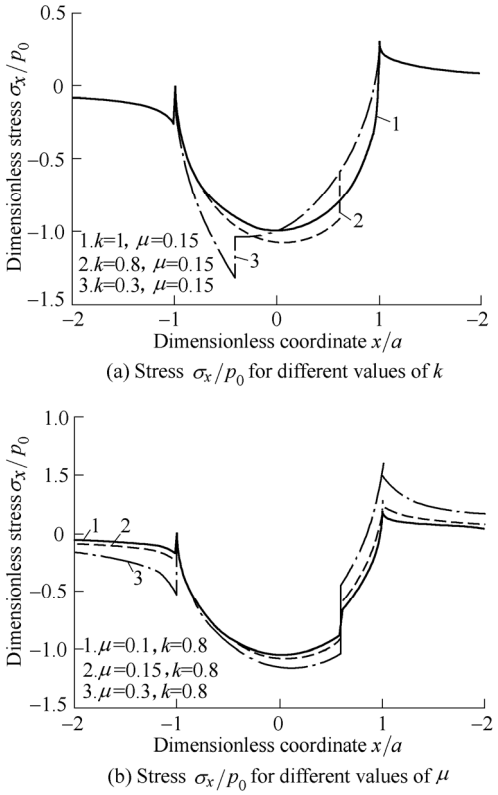

Fig. 6. Effects of k and μ on stress σ_x/p_0

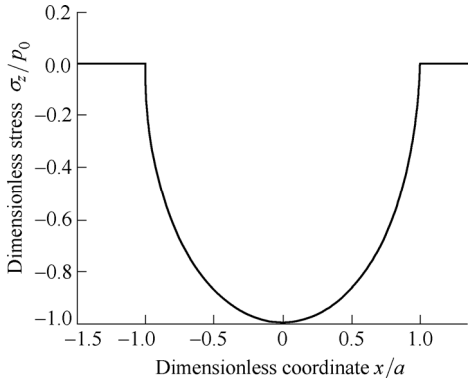

Fig. 7. Effects of k and μ on stress component σ_z/p_0

However, the parameters k and μ have no effect on the stress σ_z/p_0 of the rolling contact examined in the present study. Fig. 7 shows the results for k=0.8, μ=0.15, and y/b=0. As also shown in Fig. 8(a), for fixed values of μ= 0.15 and y/b=0, the stick region covers the entire contact area, and there is no stress mutation when k=1. Moreover, with decreasing value of k, the width of the stick region decreases while the stress τ_{xz}/p_0 increases. Furthermore, Fig. 8(b) shows that, for a fixed value of k=0.8, the tangential stress τ_{xz}/p_0 acting on the entire contact surface increases with increasing value of μ, and mutation is more obvious.

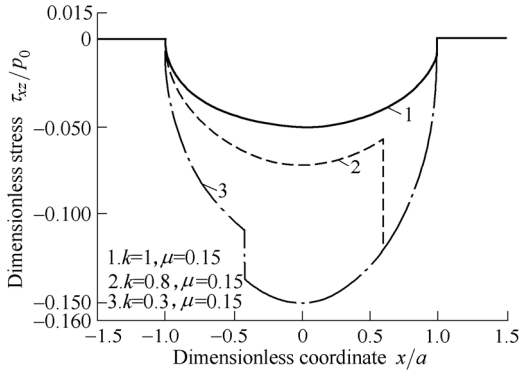

(a) Stress τ_{xz}/p_0 for different values of k

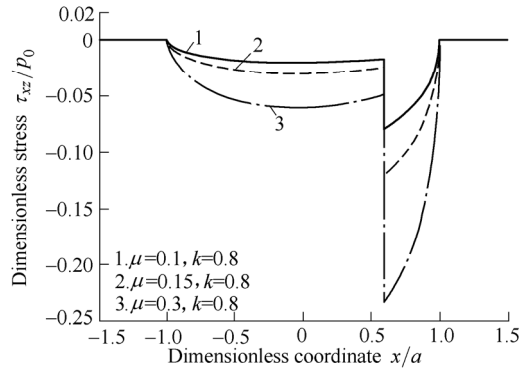

(b) Stress τ_{xz}/p_0 for different values of μ

Fig. 8. Effects of k and μ on stress component τ_{xz}/p_0

5 Conclusions

(1) The rolling contact area generally is comprised by stick and slip regions, and the surface stress component σ_x in the area is compressive in the rolling direction and tensile in the reverse direction. In addition, the amplitude of the compressive stress is greater than that of the tensile stress. With regard to σ_x and τ_{xz}, they have large gradients along the boundary between the stick and slip regions, and they should therefore be considered in the numerical prediction of fatigue and analysis of failure.

(2) With regard to the effect of the contact coefficient k on the stress components, with decreasing value of k, the scope of the stick region decreases and σ_x and τ_{xz} increase. However, the increase in the amplitude is not significant, and k is therefore not important factor in the analysis of the stress in the absence of a strict requirement. k has no effect on σ_z.

(3) With increasing value of the friction coefficient μ, σ_x and τ_{xz} increase and the stress gradient also increases. From the perspective of service life, this is beneficial to reducing the friction coefficient properly.

(4) A new method for calculating the stress of three-dimensional non-conforming rolling contact between a sphere and a cone is developed and the equations for analyzing the stress components are derived. The results of this study provide a foundation for the further study of friction, wear, and fatigue.

References

[1] FROLOV K V. *Modern tribology*: *results and perspectives*[M]. Moscow: LKI, 2007.

[2] PANDIYARAJAN R, STARVIN M S, GANESH K C. Contact stress distribution of large diameter ball bearing using Hertzian elliptical contact theory[C]//*Proceedings of International Conference on Modeling Optimization and Computing*, Kumarakoil, INDIA, 2012, 38: 264–269.

[3] FISCHER F D, WIEST M. Approximate analytical model for Hertzian elliptical wheel/rail or wheel/crossing contact problems[J]. *Journal of Tribology*, *Transactions ASME*, 2008, 138(4): 887–889.

[4] ANTOINE J F, VISA C, SAUVEY C, et al. Approximate analytical model for Hertzian elliptical contact problems[J]. *Journal of Tribology*, *Transactions ASME*, 2006, 128(3): 660–664.

[5] SACKFIELD A , HILLS D A. Some useful results in the classical Hertzian contact problem[J]. *Journal of Strain Analysis for Engineering Design*, 1983, 18(2): 101–105.

[6] SACKFIELD A , HILLS D A. Some useful results in the tangentially loaded Hertzian contact problem[J]. *Journal of Strain Analysis for Engineering Design*, 1983, 18(2): 107–110.

[7] ZHUPANSKA O I, ULITKO A F. Contact with friction of a rigid cylinder with an elastic half-space[J]. *Journal of the Mechanics and Physics of Solids*, 2005, 53(5): 975–999.

[8] GOODMAN L E. Contact stress analysis of normally loaded rough spheres[J]. *Journal of Applied Mechanics*, *Transactions ASME*, 1962, 29(9): 515–522.

[9] SPENCE D A. Self similar solutions to adhesive contact problems with incremental loading[C]//*Proceeding of the Royal Society of London*, *Series A: Mathematical and Physical Sciences*, London, UK, 1968, 305(1480): 55–80.

[10] JOHNSON K L. *Contact mechanics*(*9th printing*)[M]. UK: Cambridge University Press, 2003.

[11] SHCHERBAKOV S S. Spatial stress-strain state of tribofatigue system in roll-shaft contact zone[J]. *Strength of Materials*, 2013, 45(1): 35–43.

[12] CARTER F W. On the action of locomotive driving wheel[C]// *Proceedings of the Royal Society of London*, London, UK, 1926, 112: 151–157.

[13] FROMN H. Berechnung des schlupfes beim rollen deformeirbarer scheibem[J]. *Zeitschrift fur Mathematik und Mechanik*, 1927, 7: 27–58.

[14] KALKER J J. *Three-dimensional elastic bodies in rolling contact*[M]. The Netherlands: Dordrecht, Kluwer Academic Publishers, 1990.

[15] WANG Wenjian, GUO Jian, LIU Qiyue. Effect of track structure parameters on rolling contact stresses of wheel/rail[J]. *Journal of Mechanical Engineering*, 2009, 45(5): 39–44. (in Chinese)

[16] ZHANG Shurui, LI Xia，WEN Zefeng, et al. Theory and numerical method of elastic bodies in rolling contact with curve contact area[J]. *Engineering Mechanics*, 2013, 30(2): 30–37. (in Chinese)

[17] TAO Gongquan, LI Xia, WEN Zefeng, et al. Comparative analysis of two algorithms for wheel-rail contact stress[J]. *Engineering Mechanics*, 2013, 30(8): 229–235. (in Chinese)

[18] LI Wei, WEN Zefeng, JIN Xuesong, et al. Numerical analysis of rolling-sliding contact with the frictional heat in rail[J]. *Chinese Journal of Mechanical Engineering*, 2014, 27(1): 41–49.

[19] JIN Xuesong, WEN Zefeng, ZHANG Weihua. Analysis of contact stresses of wheel and rail with two types of profiles[J]. *Journal of Mechanical Engineering*, 2004, 40(2): 5–11. (in Chinese)

[20] BOGDANSKi S, OLZAK M, STUPNICKI J. Numerical stress analysis of rolling contact fatigue cracks[J]. *Wear*, 2006, 191(1–2): 14–24.

[21] WEN Zefeng, WU Lei, JIN Xuesong, et al. Three-dimensional elastic-plastic stress analysis of wheel-rail rolling contact[C]// *Proceedings of the 8th International Conference on Contact Mechanics and Wear of Rail/Wheel Systems*, Florence, Italy, 2011,

271(1–2): 426–436.
[22] YANG Guoqing, HONG Jun, ZHU Linbo, et al. Three-dimensional finite element analysis of the mechanical properties of helical thread connection[J]. *Chinese Journal of Mechanical Engineering*, 2013, 26(3): 564–572.
[23] DU Xiaoming, REN Jindong, SANG Chunlei et al. Simulation of the interaction between driver and seat[J]. *Chinese Journal of Mechanical Engineering*, 2013, 26(6): 1234–1242.
[24] KUDRA G, AWREJCEWICZ J. Approximate modelling of resulting dry friction forces and rolling resistance for elliptic contact shape[J]. *European Journal of Mechanics A-Solids*, 2013, 42: 358–375.
[25] KUMINEK T, ANIOLEK K. Methodology and verification of calculations for contact stresses in a wheel-rail system[J]. *Vehicle System Dynamics*, 2014, 52(1): 111–124.
[26] AALAMI M R, ANARI A, SHAFIGHFARD T, et al. A robust finite element analysis of the rail-wheel rolling contact[J]. *Advances in Mechanical Engineering*, 2013, 2013: 1–9.
[27] MAOUCHEN N, MAITOUMAM M H, VAN K D. On a new method of evaluation of the inelastic state due to moving contacts[J]. *Wear*, 1997, 203-204(3): 139–147.
[28] XU Biqiang, JIANG Yanyao. Elastic-plastic finite element analysis of partial slip rolling contact[J]. *Journal of Tribology*, *Transactions of ASME*, 2002, 124(1): 20–26.
[29] LEE D H, SEO J W, KWON S J, et al. Three-dimensional transient rolling contact analysis of similar elastic cylinders[C]// *Proceedings of 11th International Conference on the Mechanical Behavior of Materials*, Como, Italy, 2011, 10: 2633–2638.
[30] ETSION I, LEVINSON O, HALPERIN G, et al. Experimental investigation of the elastic-plastic contact area and static friction of a sphere on flat[J]. *Journal of Tribology*, *Transactions of ASME*, 2005, 127(1): 47–50.
[31] POPOV V L. *Contact mechanics and friction: physical principles and applications*[M]. Germany: Springer, 2011.

Biographical notes

ZHAO Yanling, born in 1963, is currently a professor at *School of Mechanical and Power Engineering, Harbin University of Science and Technology, China.* She received her bachelor degree from *Harbin Institude of Technology, China*, in 1986 and received her master degree and PhD degree from *Harbin University of Science and Technology, China,* in 1989 and 2008, respectively. Her current research interests include friction and wear study, mechanical structure design and system dynamics.
Tel: +86-18646491009; E-mail: zhaoyanling@sina.com

XIA Chengtao, born in 1988, is currently a master candidate at *School of Mechanical and Power Engineering, Harbin University of Science and Technology, China.* He received his bachelor degree from *Shandong University of Technology, China,* in 2012. His research interests include elastic mechanics and contact theory.
Tel: +86-18646276392; E-mail: xiachengtao1020@126.com

WANG Hongbo, born in 1988, is a technologist at *Shenyang Aerospace Mitsubishi Motors Engine Manufacturing Co., Ltd, China.* She received her master degree from *Harbin University of Science and Technology, China,* in 2015. Her research interests include elastic mechanics and contact theory.
Tel: +86-13945136103; E-mail: wanghongbolinlin@163.com

XUAN Jiaping, is currently a technologist at *Shenyang Aerospace Mitsubishi Motors Engine Manufacturing Co., Ltd, China.* He recieve his master degree from *Harbin University of Science and Technology, China,* in 2014. His research interests include dynamics simulation and numerical analysis.
Tel: +86-18802410724; E-mail: xuanjiaping0928@163.com

XIANG Jingzhong, born in 1962, is currently a professor at *School of Mechanical and Power Engineering, Harbin University of Science and Technology, China* and a vice president of *Mechanical Design Teaching Research Association of Heilongjiang Province, China.* He received his master degree from *Harbin University of Science and Technology, China,* in 2003. His research interests include mechanical and electrical integration and motion control technology.
Tel: +86-13603607262; E-mail: 442050804@qq.com

LIU Xianli, born in 1961，is currently a professor and the president at *School of Mechanical and Power Engineering, Harbin University of Science and Technology, China.* He received his PhD degree from *Harbin Institude of Technology, China,* in 1999. His research interests include clean cutting, multimedia cutting database technology and image technology.
Tel: +86-13945111601; E-mail: 13945111601@139.com

SU Xiangguo, born in 1977, is currently an associate professor at *School of Mechanical and Power Engineering, Harbin University of Science and Technology, China.* He received his master degree from *Harbin Institude of Technology, China*, in 2000. His research interests include fatigue and failure analysis.
Tel: +86-15645036966; E-mail: 78405229@qq.com